Capacity Limits of C+L Metro Transport Networks Exploiting Dual-Band Node Architectures

Robert Emmerich[(1)], António Eira[(2)], Nelson Costa[(2)], Pablo Wilke Berenguer[(1)], Colja Schubert[(1)], Johannes Karl Fischer[(1)], João Pedro[(2,3)]
(1) Fraunhofer Institute for Telecommunications Heinrich-Hertz-Institute, Einsteinufer 37, 10587 Berlin, Germany
(2) Infinera Portugal, R. da Garagem 1, 2790-078 Carnaxide, Portugal
(3) Instituto de Telecomunicações, Instituto Superior Técnico, Av. Rovisco Pais 1, 1049-001 Lisboa, Portugal
robert.emmerich@hhi.fraunhofer.de

Abstract: We investigate capacity upgrade of metro networks using differentiated node architectures for C+L-bands. The combination of experimental results and network simulations highlights scenarios where low-cost unamplified L-band extensions can be leveraged for maximum capacity.

1. Introduction

Metro Area Networks (MANs) are at the forefront of the capacity crunch associated with supporting 5G service requirements. Simultaneously, cost-per-bit reduction is a priority for operators, making the reuse of the existing fiber plant essential. In this scope, extending transmission beyond the C-band becomes an appealing solution for cost-efficient capacity upgrade in MANs [1]. In the short run, the L-band is the most promising option for fiber capacity extension, given favorable fiber transmission properties that enable practical deployment of extra capacity [2-3]. However, typical L-band deployments rely either on duplicating the line system (node degrees and amplifiers), or replacing the existing plant with an integrated infrastructure, e.g. with C+L amplifiers [2].

The physical architecture of legacy MANs typically reflects their connectivity requirements: i.e. ring/horseshoe topologies where a set of metro aggregation nodes communicate directly with a hub node facing the core segment. This simple hub-and-spoke traffic pattern does not require heavy meshed connectivity between arbitrary nodes, which allows using simpler optical switching structures based on fixed optical add/drop multiplexers (FOADMs) or on filterless solutions [4]. However, the spread of edge computing tends to split MAN traffic requirements into bulk north-south flows directed to/from the core, and less predictable mesh patterns that depend on each specific service's requirements, as well as the need to direct flows wherever storage/compute resources are more readily available [5]. Given this functional split, it is worth evaluating the different options for deploying L-band capabilities in MANs, considering how the node architecture in each band can be practically and cost-effectively geared towards differentiated traffic requirements. To this effect, we perform experimental evaluations to assess the viability of L-band transmission with unamplified and amplified solutions. Using these results as dimensioning rules, we verify through network simulation the MAN system capacity of different C+L-band architectural combinations.

2. Dual C+L-band Architecture

The considered baseline MAN architecture is based on a chain/horseshoe topology with a hub node and several tributary metro aggregation nodes, as depicted in Fig. 1. Transmission in the C-band is supported by various node architecture options, which may be based on FOADMs, reconfigurable OADMs (ROADMs), or filterless drop & waste solutions. Each offers different trade-offs between capacity/flexibility and cost/complexity of the designs [4]. Adding L-band transmission to such networks can be accomplished by using C/L couplers/splitters at the egress/ingress degrees to create independent express and add/drop structures per band. This dual architecture allows the L-band to be designed according to specific traffic and/or cost requirements, while also enabling it to complement any potential connectivity limitations present in legacy C-band architectures. In this work, we evaluate the addition of a filterless L-band in two flavors: (1) An amplified L-band, which adds more available spectrum for channels (Chs) be-

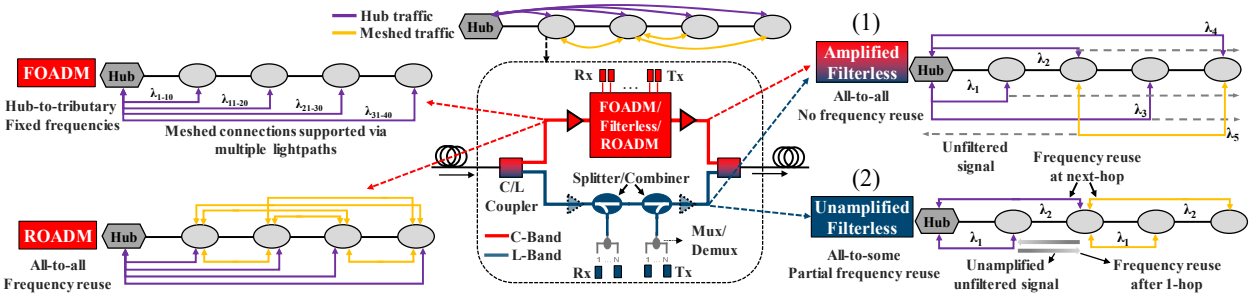

Fig.1 Dual-band node architecture configurations in MANs for C- and L-band.

tween any two nodes but expending the frequency across the entire network. (2) An unamplified solution, where L-band connectivity is limited to adjacent or near-adjacent node-pairs, and the absence of amplification is leveraged to reuse the same frequency multiple times in the network. The latter provides a simple and very low-cost capacity upgrade for MANs with dedicated capacity for short lightpaths between aggregation nodes, albeit with a more challenging optical performance management. While the feasibility of amplified filterless L-band transmission has been previously demonstrated [2], the practical suitability of the unamplified solution must be validated in terms of: (a) maximum achievable span lengths, and (b) the maximum homodyne crosstalk level from upstream Chs that allows frequency reuse in a downstream span. In the remainder of the paper, we experimentally evaluate these design limitations and analyze their impact in terms of achievable network-wide capacity.

3. Experimental Setup and Design Rules

First, we experimentally assess the potential of the L-band for unamplified transmission of 100 Gb/s dual-polarization (DP) quadrature phase-shift keying (QPSK) and 200 Gb/s DP 16-ary quadrature-amplitude modulation (16-QAM) with the setup shown in Fig. 2a indicated by blue dotted lines. The channel under test (CUT) is generated from an external cavity laser (ECL, 1586.2 nm) using a DP-IQ modulator that is driven by a digital-to-analog-converter (DAC) via 4 driver amplifiers. The DAC waveforms (roll-off 0.1) are created with data-aided digital signal processing (DSP) as in [2]. The power (P) per Ch at the output of the transmitter (Tx) is -4.6 dBm for QPSK and -6.1 dBm for 16-QAM, respectively. Since homodyne in-band crosstalk can be an important limitation in filterless MANs [6], we evaluate it by generating a copy of the signal with a 3 dB splitter, that is decorrelated by a 100 m optical fiber (~500 ps delay), attenuated and added back to the transmitted signal using another 3 dB coupler. The optical power (P_{Rx}) reaching the intradyne coherent receiver (ICR) is varied from -11 dBm to -33 dBm for QPSK and from -13 dBm to -27 dBm for 16-QAM in order to measure the sensitivity of the receiver (Rx). In the ICR, the signal is mixed with the local oscillator (LO) ECL (16.0 dBm) and the single ended outputs of the ICR are digitized using a real-time sampling scope (RTO). The offline DSP at the Rx uses training-aided carrier-frequency offset compensation and equalization [2]. This is followed by a blind phase search and a second, real-valued 4x4 MIMO equalizer (101 taps, T-spaced, decision-directed least-mean square equalizer). Finally, the bit-error ratio (BER) is counted. The sensitivity penalty (based on 0 dB @ -63 dB crosstalk level) of the Rx is presented in Fig. 2c. If a 16-QAM signal (solid line, blue diamonds) is transmitted at the soft-decision (SD) forward error correction (FEC) threshold (BER = 2e-2) with a crosstalk level of -20 dB (leading to 1 dB Rx penalty) a crosstalk tolerance reduction exceeding 5 dB is observed with respect to QPSK (dotted line, blue diamonds). As 16-QAM is less tolerant to homodyne in-band crosstalk, interfering power per Ch (P_{ch}) must be 20 dB below signal power for negligible impact of crosstalk (compared to 14 dB for QPSK). If for 16-QAM the hard-decision (HD) FEC threshold is used instead (BER = 3.8e-3), the interfering P_{ch} must be about 23 dB below signal power at the same penalty of 1 dB.

As second step, the full setup in Fig. 2a is used to measure the performance over 80 km with interferers in the C- and the L-band without the back-to-back (btb) part in the blue dotted lines. The interfering loader Chs (80 in the C- and 15 in the L-band) are created with EDFAs and wavelength selective switches (WSS) in both bands (L-band WSS kindly provided by Finisar). After each WSS an EDFA is used to compensate for WSS loss and variable optical attenuators (VOA) set a fixed P_{ch} of 0 dBm in the C-band and a variable P_{ch} from 6 dBm to -10 dBm in the L-band. The optical spectra after the first C/L coupler for 0 dBm at all Chs is shown in Fig. 2b. After 80 km standard single mode fiber (SSMF, 16 dB loss) a second C/L coupler is used to split the two bands. The L-band is passed to a VOA to change P_{RX} from -17 dBm to -34 dBm. The BER is determined as described previously. The corresponding transmission results over P_{RX} for QPSK and 16-QAM are shown in Fig. 2d. P_{ch} for all interferers and the CUT in the L-band is varied from 6 dBm to -10 dBm. For the transmission of QPSK only minor penalties are observed at high P_{ch}. The BER for 16-QAM shows a significant degradation for P_{ch} higher than 3 dBm. Furthermore, the achievable P_{RX} into the Rx is limited by the transmission loss and therefore not all targeted P_{RX} can be achieved.

Based on these results, the design rules for lightpath deployment over the unamplified filterless L-band are de-

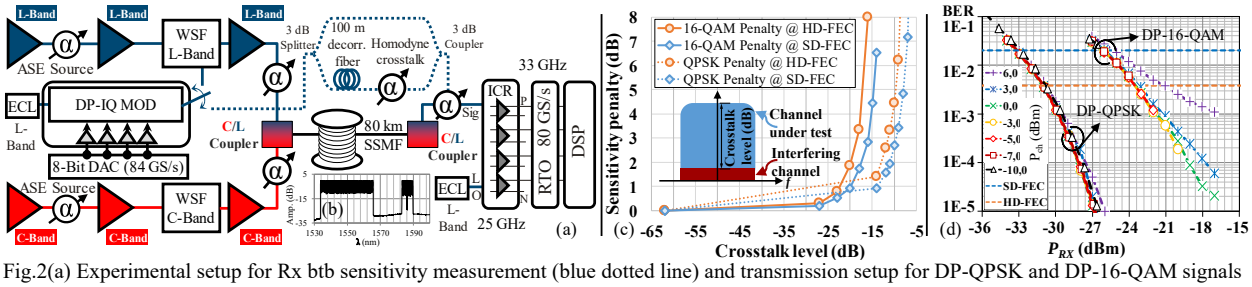

Fig.2(a) Experimental setup for Rx btb sensitivity measurement (blue dotted line) and transmission setup for DP-QPSK and DP-16-QAM signals in L-band, (b) the transmitted spectrum after C/L coupler, (c) sensitivity penalty of Rx btb vs. crosstalk at HD- and SD-FEC thresholds with a depiction of the crosstalk level as insert and (d) the transmission results (BER) vs. received power after 80 km SSMF.

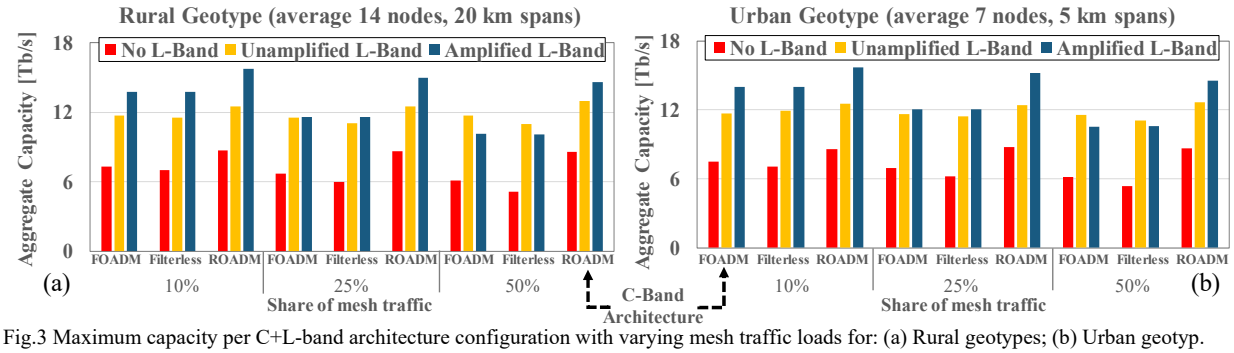

Fig.3 Maximum capacity per C+L-band architecture configuration with varying mesh traffic loads for: (a) Rural geotypes; (b) Urban geotyp.

rived. We assume 3.5 dB insertion losses (IL) in splitters/combiners, and 0.5 dB for C/L couplers. The optimum launch power is 0 dBm and SD-FEC is used. Based on Fig. 2c and 2d, the penalty-free crosstalk sensitivity thresholds for QPSK and 16-QAM are -33 and -26 dBm, respectively. Assuming a 5 dB IL in the mux/demux add/drop, we find that QPSK Chs support transmission over a single hop with up to 15 dB attenuation (roughly 75km), or over two-hops with a cumulative span loss of 7 dB (35 km). These values hold regardless of frequency reuse in adjacent links, as in-band crosstalk effects are manageable with interfering Ch powers up to 8 dB above the Rx sensitivity. For 16-QAM Chs, only one-hop with up to 8 dB loss (40 km) is bridgeable. Furthermore, a Ch at the minimum Rx sensitivity threshold for 16-QAM introduces unacceptable crosstalk levels in the express branch for another Ch added over the same frequency. Hence, 200 Gb/s Chs may only be deployed over single hops with less than 8 dB loss and the same frequency cannot be reused in the immediately adjacent links.

4. Network Simulation and Results

In order to analyze the potential of mixing different C+L-band architectures, we performed simulations to verify the capacity limits of each configuration. We evaluated combinations of a 40-Chs ROADM/FOADM /filterless C-band by itself, and complemented with a filterless amplified or unamplified L-band (also 40 Chs). For the latter, the Ch assignment restrictions derived previously apply. The simulation sequentially generates traffic demands between 1 and 50 Gb/s and assigns them using the least-cost path over an auxiliary graph modeling existing/potential lightpaths (100 or 200 Gb/s) in both bands [7]. The investigated scenarios include rural- and urban-type horseshoes (details in Fig. 3 headers). Furthermore, we assess different traffic patterns by varying the share of "mesh" demands that do not start/end at the hub node. The results are averaged (avg) over 100 simulations for each scenario. Fig. 3a and 3b show the achievable capacity in rural- and urban-type networks, respectively. Overall, the capacity unlocked by the unamplified L-band is larger in scenarios with more meshed demands, and where the C-band is less able to support that meshed traffic. This is naturally the case for a FOADM C-band, but also for filterless designs where frequencies are quickly expended supporting all possible node-pairs. A FOADM/filterless C-band with 50% mesh traffic supports an avg of 91% more traffic with an unamplified L-band, vs. 82% with the amplified one. In these scenarios, the ability to reuse frequencies outweighs the need to establish longer lightpaths, albeit requiring more transponders. With a ROADM-based C-band, mesh traffic can be efficiently served in this band, and thus an amplified L-band is a better complement by providing transparent capacity for longer links (on avg 20% more capacity than with the unamplified design). These findings are quite similar in both the rural and urban geotypes, suggesting the performance of unamplified Chs covers both ends of the metro aggregation application range for 1- and 2-hop connections.

5. Conclusion

We evaluated MAN configurations deploying C+L channels with differentiated node architectures per band. The experimental assessment of unamplified filterless L-band transmission revealed its usefulness for metro-sized spans, enabling full or partial frequency reuse depending on the modulation format employed. Network simulation further demonstrated that this option can provide a sizeable capacity extension at lower costs, particularly when the legacy C-band architecture is limited in its ability to provide meshed transparent connectivity.

6. Acknowledgements

This work was partially supported by the H2020 Metro-Haul project under grant agreement number 761727.

References

[1] Fischer et al., "Maximizing the capacity of installed optical fiber infrastructure via wideband transmission", ICTON, Tu.B3.3, 2018
[2] Paolucci et al., "Filterless optical WDM metro networks exploiting C+L band", ECOC, Tu.1.D.5, 2018
[3] Srivastava et al., "Ultradense WDM transmission in L-band", IEEE PTL, vol. 12 (11), pp. 1570-1572, Nov. 2000
[4] Eira et al., "On the capacity and scalability of metro transport architectures for ubiquitous service delivery", ICTON, Mo.B3.5, 2018
[5] Askari et al., "Virtual network function placement for dynamic service chaining in metro-area networks", ONDM, pp.136-141, 2018
[6] Winzer et al., "Penalties from in-band crosstalk for advanced optical modulation formats", ECOC, Tu.5.B.7, 2011
[7] Zhu et al, "A novel generic graph model for traffic grooming in heterogeneous WDM mesh networks", IEEE/ACM ToN, vol.11 (2), 2003